



Effects of different carbon sources on the compressive properties of in situ high-volume-fraction $\text{TiC}_x/2009\text{Al}$ composites

L. Wang, F. Qiu, S.-L. Shu, Q.-L. Zhao & Q.-C. Jiang

To cite this article: L. Wang, F. Qiu, S.-L. Shu, Q.-L. Zhao & Q.-C. Jiang (2016) Effects of different carbon sources on the compressive properties of in situ high-volume-fraction $\text{TiC}_x/2009\text{Al}$ composites, Powder Metallurgy, 59:5, 370-375, DOI: [10.1080/00325899.2016.1251061](https://doi.org/10.1080/00325899.2016.1251061)

To link to this article: <http://dx.doi.org/10.1080/00325899.2016.1251061>



Published online: 17 Nov 2016.



Submit your article to this journal [↗](#)



Article views: 37



View related articles [↗](#)




View Crossmark data [↗](#)



Citing articles: 1 View citing articles [↗](#)

Effects of different carbon sources on the compressive properties of *in situ* high-volume-fraction TiC_x/2009Al composites

L. Wang¹, F. Qiu^{*1}, S.-L. Shu², Q.-L. Zhao ¹ and Q.-C. Jiang^{*1}

Effects of carbon sources, i.e. carbon nanotubes (CNTs), graphite, carbon black (C-black), on synthesised TiC_x size, shape and compressive properties of *in situ* 40–60 vol.-% TiC_x/2009Al composites were investigated. When CNTs and C-black were used, the synthesised TiC_x with particle sizes of 0.08–1 and 0.9–5 μm, respectively, was spherical or nearly spherical in shape, while graphite was used, the synthesised TiC_x with particles sizes of 0.2–2 μm was octahedral or spherical in shape. The yield strength ($\sigma_{0.2}$), ultimate compression strength (σ_{UCS}) and hardness of TiC_x/2009Al composites all increased with increasing TiC_x content, while the plastic strain (ϵ) decreased. The $\sigma_{0.2}$, σ_{UCS} , ϵ and hardness of 60 vol.-% TiC_x/2009Al composites fabricated by using CNTs were 722 MPa, 946 MPa, 3.2% and 260 ± 10 Hv, respectively. The strength increase of the composites resulted from finer-sized TiC_x particles with spherical shape.

Keywords: Different carbon sources, TiC_x particles, Morphology, Composites, Compressive properties

Introduction

Metal matrix composites (MMCs) reinforced with high-volume-fraction (>30%) ceramic particles, due to good combination of electrical and thermal conductivity as well as dimensional stability, are found to be potential materials for electronic packaging.^{1–4} However, the fact that the high-volume-fraction reinforcements usually lead to the defects such as cavities and cracks, makes the fabrication of such composites more difficult.^{3,5} Works on the fabrication of high-volume-fraction ceramic particles-reinforced MMCs by both *ex situ* and *in situ* methods have been done, including powder metallurgy,^{1,6} pressure infiltration,^{7,8} combustion synthesis,^{4,9,10} etc. As known, in contrast to the *ex situ* methods, the *in situ* methods which takes the advantages of higher purity of the products and cleaner particle/matrix interface is more beneficial to the mechanical properties of the composites.¹¹

Combustion synthesis, as a more technically simple and energy efficient method, has been applied to prepare ceramic particles.¹² Among numerous ceramic candidates, TiC_x, because of its high hardness, modulus and thermal stability, is an attractive ceramic material for use as a reinforcing phase in Al matrix composites (AMCs).¹³ Generally, the strength of MMCs is directly controlled by the

size, shape and content of the reinforcements as well as the bonding strength between matrix and reinforcement.^{14–16} When finer-sized ceramic particles, especially nano-sized particles, with proper shape are dispersed uniformly in the metal matrix, the MMCs will exhibit excellent mechanical properties. Considerable efforts on combustion synthesis of TiC_x with different content, shape and size from Al–Ti–C system have been made, of which different carbon sources are used. In fact, carbon sources with different structure have great effects on the synthesised TiC_x particles size and shape. For example, by using CNTs as carbon source, Jin *et al.*¹⁷ synthesised 20 wt-% nano-sized TiC_x particles with octahedral shape. Song *et al.*¹⁸ fabricated 60–80 wt-% TiC_x/Al composites by self-propagating high-temperature synthesis of Al–Ti–C-black system. They found that the synthesised TiC_x with particles size in the range of 0.5–2 μm was spherical in shape, and meanwhile, the particles size decreased with addition of Al. Besides that, by using graphite and amorphous carbon as carbon source, Choi and Rhee¹⁹ investigated the effect of structure of carbon source on the reaction mechanism and reactivity in the combustion synthesis of TiC_x. However, these studies mainly focus on the formation mechanism, size, morphology, etc., of synthesised TiC_x particles, but no mechanical properties of the composites are given. Investigations of the effects of different carbon sources on the compression properties of high-volume-fraction TiC_x particles-reinforced AMCs have rarely been reported.

In this paper, 40, 50 and 60 vol.-%TiC_x/2009Al composites were fabricated via the combined method of combustion synthesis and vacuum hot press. Meanwhile, effects of different carbon source (CNTs, graphite and C-black)

¹Department of Materials Science and Engineering, Key Laboratory of Automobile Materials, Ministry of Education, Jilin University, No. 5988 Renmin Street, Changchun 130025, People's Republic of China

²State Key Laboratory of Luminescence and Applications, Changchun Institute of Optics, Fine Mechanics and Physics, Chinese Academy of Sciences, Changchun 130012, People's Republic of China

*Corresponding author, email jqc@jlu.edu.cn (Q.-C. J.); qjufeng@jlu.edu.cn (F. Q.)

on synthesised TiC_x size, morphology and compression properties of the composites were investigated.

Sample preparation and testing

Materials

The raw materials were Ti powders (>99.5% purity, ~48 μm), CNTs (10–20 nm in diameter and 20–100 μm in length), graphite (>99.9% purity, ~48 μm), C-black (>99.9% purity, ~40 nm) and 2009Al alloy powders (~75 μm). The chemical composition (in wt-%) of 2009Al consisted mainly of 3.7 Cu, 1.3 Mg, 0.25 Si, 0.05 Fe and Bal. Al.

Specimen processing

First, Ti powders and carbon powders (CNTs, graphite and C-black) with a molar ratio of 1:1 were mixed with 40, 50 and 60 vol.-% 2009Al alloy powders. The reactants were mixed sufficiently by ball milling for 8 h and then condensed into the cylindrical compacts (Φ28 × 35 mm) with green densities of ~65 ± 2% of theoretical. Then, the reactants were put into a self-made vacuum furnace and heated in a vacuum atmosphere. The temperature was monitored by W5-Re26 thermocouples. When the temperature measured by the thermocouple rapidly rose, indicating that the sample should be ignited. The sample was quickly pressed while it was still hot and soft.

Test methods

The phase constitution of the synthesised composites were characterised by X-ray diffractometry (XRD, Rigaku D/Max 2500PC, Tokyo, Japan) with Cu Kα radiation utilising a scanning speed of 4°/min. The morphology of TiC_x particles extracted from aluminium matrix with 5 vol.-% HCl-distilled water solution were observed using a field

emission scanning electron microscope (FESEM, JSM 6700F, Tokyo, Japan). The microstructure of the composites was studied by using scanning electron microscopy (SEM, Evo18, Carl Zeiss, Oberkochen, Germany). Micro-hardness was measured by a Vickers hardness tester (Model 1600-5122VD, Chicago, USA) with a static load of 3 N and a dwell time of 10 s. The compression properties tests were carried out with a servo hydraulic materials testing system (MTS, MTS 810, Minneapolis, USA) at a strain rate of 3 × 10⁻⁴ s⁻¹.

Results and discussion

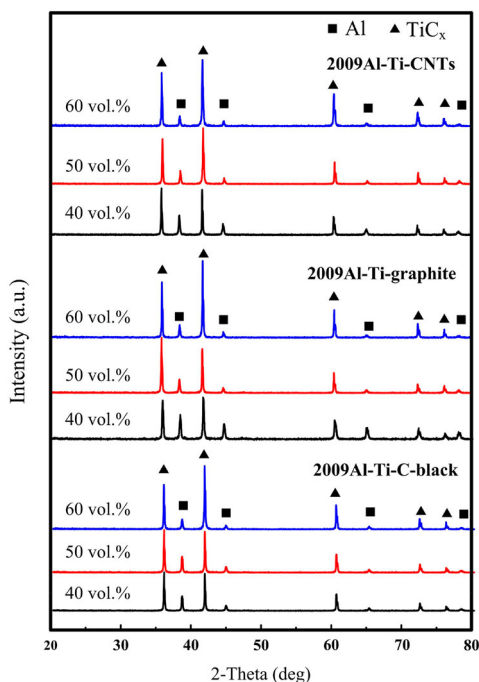
XRD analysis

Figure 1*a–c* shows XRD patterns of the synthesised 40–60 vol.-% TiC_x/2009Al composites fabricated by using CNTs, graphite and C-black as carbon source. It can be observed that in addition to the main phase constitutions, i.e. TiC_x and α-Al phase, no other phase is detected in these samples, indicating that the combustion reaction proceeds more thoroughly.

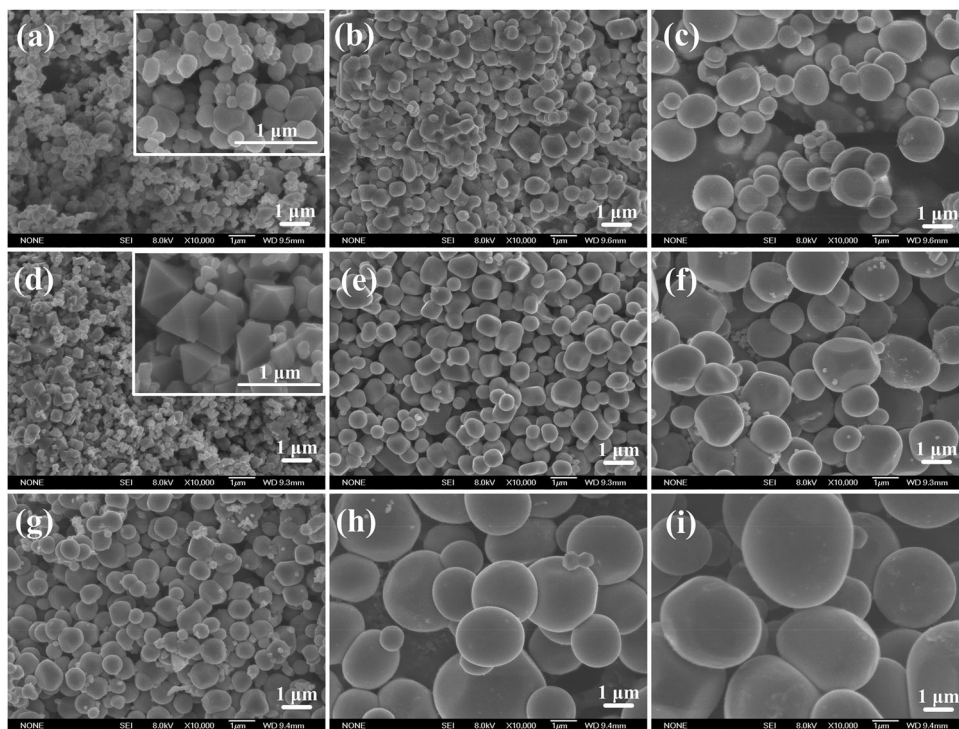
Morphology of the synthesised TiC_x particles

The FESEM images of the extracted samples of 40–60 vol.-% TiC_x/2009Al composites fabricated by using CNTs, graphite and C-black as carbon source are shown in Fig. 2*a–i*. It can be seen that with increasing TiC_x content, all of the TiC_x particles size increases gradually. When CNTs are used, as showed in Fig. 2*a–c*, with TiC_x content increases from 40 to 60 vol.-%, the TiC_x particles size is in the range of 0.08–1 μm. Meanwhile, the synthesised TiC_x particles are generally spherical- or spheroidal in shape. As shown in Fig. 2*d–f*, when graphite is used, the TiC_x particles size is in the range of 0.2–2 μm. The synthesised 40 vol.-% TiC_x is octahedral in shape, while synthesised 50 and 60 vol.-% TiC_x are spherical in shape. When C-black is used, as shown in Fig. 2*g–i*, the synthesised TiC_x particles with sizes in the range of 0.9–5 μm are spherical- or spheroidal in shape. In contrast to graphite and C-black, TiC_x particles synthesised by using CNTs as carbon source have the smallest size, especially the 40 vol.-% TiC_x particles size is ~0.08 μm.

In the Al–Ti–C systems, the reaction between Al and Ti to form Al₃Ti happens first, which is mainly controlled by diffusion.²⁰ During the heating, the Al–Ti liquid forms. The carbon then diffuses into the Al–Ti liquid, and when the concentration of [Ti] and [C] in Al–Ti–C ternary liquid phase is high enough for reactions between [Ti] and [C] to occur, TiC_x will be synthesised.^{21–23} In this process, on one hand, the diffusion of carbon in the molten Al is a key step to form TiC_x. Compared with finer-sized carbon source, the diffusion of large-sized carbon source is slower, and more heat will be needed when large-sized carbon source dissolves, which finally causes decrease in the combustion temperature in Al–Ti–C systems.¹⁹ It have been pointed out that the stoichiometry of TiC_x, influenced by combustion temperature, has great effect on its morphology. The synthesised TiC_x particles tend to be spherical in shape at high combustion temperature. Owing to the limited dissolution of carbon at low combustion temperature, the synthesised TiC_x particles are likely to be octahedral in shape.^{17,24,25} On the other hand, as the addition of Al content increases, the



1 XRD patterns of 40, 50 and 60 vol.-%TiC_x/2009Al composites fabricated by using CNTs, graphite and C-black as carbon source



2 FESEM images of the extracted samples of 40, 50 and 60 vol.-%TiC_x/2009Al composites fabricated by using a–c CNTs, d–f graphite and g–i C-black as carbon source

combustion temperature in Al–Ti–C systems decreases as well.¹⁸ With decrease in the combustion temperature, the synthesised TiC_x particles size decreases. In addition, the apparent reactivity of different carbon sources is various. In contrast to the graphite and C black, CNTs have much finer sizes. Moreover, the defects such as pentagons, heptagons and vacancies in the structure of the CNTs increase its dissolvability.²⁶ Accordingly, TiC_x particles synthesised by using CNTs have the smallest size. Although C-black possesses fine size (~40 nm), the apparent reactivity of Ti powder with CNTs and graphite seems to be higher than with amorphous C-black.¹⁹ Hence, the TiC_x particles synthesised by using C-black with spherical shape have the largest size.

Microstructure of corresponding composites

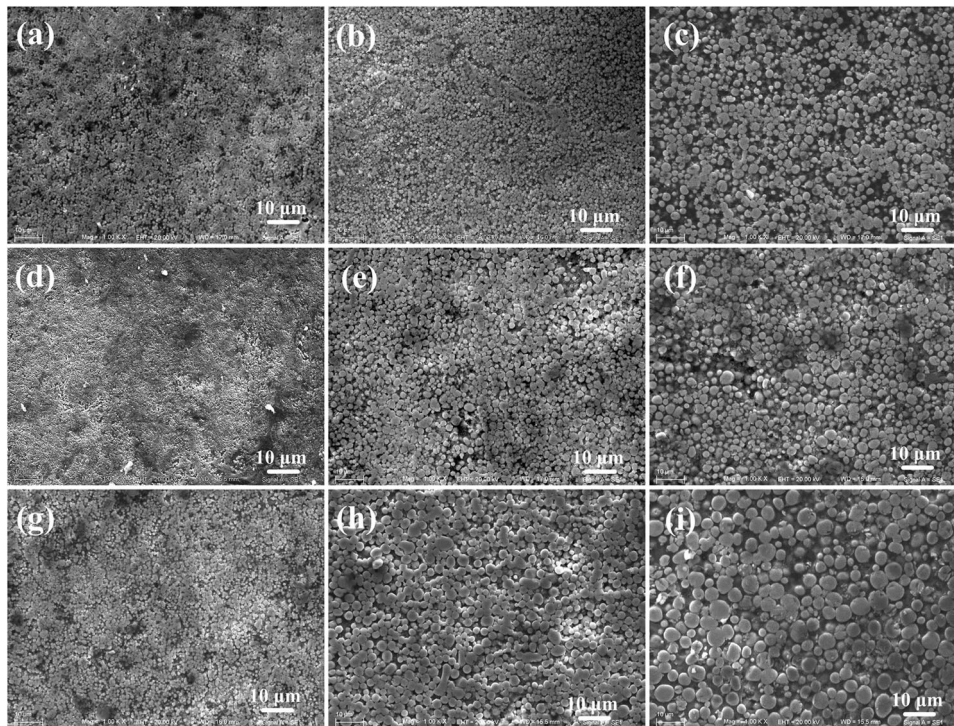
Figure 3a–i shows SEM images of the etched surfaces of 40–60 vol.-% TiC_x/2009Al composites fabricated by using CNTs, graphite and C-black as carbon source. As indicated, the composites are relatively dense and there are no obvious holes and cracks. Meanwhile, the synthesised TiC_x particles in these composites exhibit a uniform distribution in the matrix.

Compression testing

Figure 4a–c shows the compression engineering stress–strain curves of 40–60 vol.-% TiC_x/2009Al composites fabricated by using CNTs, graphite and C-black as carbon source. The compression test data is summarised in Table 1. Micro-hardness of 40–60 vol.-% TiC_x/2009Al composites is showed in Fig. 4d. Clearly, all of the yield strength ($\sigma_{0.2}$), ultimate compression strength (σ_{UCS}) and hardness of TiC_x/2009Al composites increase with increasing TiC_x content, while the plastic strain (ϵ)

decreases. Among all the investigated composites, the ones fabricated by using CNTs exhibit the highest $\sigma_{0.2}$, σ_{UCS} and hardness. Especially, the 60 vol.-% TiC_x/2009Al composites fabricated by using CNTs have the highest σ_{UCS} and hardness (~946 MPa, 260 ± 10 Hv), which are 11.4% and 3.4%, 13.4% and 7.5% higher than those of composites fabricated by using graphite (~849 MPa, 252 ± 9 Hv) and C-black (~834 MPa, 242 ± 7 Hv) as carbon sources. The increase in the σ_{UCS} and hardness of the present composites may be attributed to the existence of finer-sized TiC_x particles in its microstructure and high interfacial strengthening effect.²⁷ Moreover, Kouzeli *et al.*¹⁴ and Romanova *et al.*¹⁵ have reported that the particles with sharp corners are harmful to the composites. The stress concentration and the formation of cracks will occur at the sharp corners, which will facilitate the fracture of the composites. Therefore, the strength of 40 vol.-% TiC_x/2009Al composites fabricated by using graphite is lower than those of composites fabricated by using CNTs and C-black as carbon sources.

In addition, Tan *et al.*²⁸ fabricated 50 vol.-% SiC_p/2024Al composites by using squeeze casting technology, of which the σ_{UCS} was 520 MPa under the strain rate of $1.0 \times 10^{-3} \text{ s}^{-1}$. Ahlatci *et al.*^{8,29} fabricated the 60 vol.-% SiC_p/Al composites by the method of the pressure infiltration. Its σ_{UCS} was reported to be 340 MPa under the compression strain rate of $8.3 \times 10^{-3} \text{ s}^{-1}$. However, the σ_{UCS} of 60 vol.-%TiC_x/2009Al composites fabricated by using CNTs is 946 MPa under the compression strain rate of $3 \times 10^{-4} \text{ s}^{-1}$. The first, when CNTs are used, the synthesised TiC_x particles size is ~1 μm, which is much smaller than SiC particles in composites fabricated by Tan *et al.*²⁸ (~4 μm) and Ahlatci *et al.*^{8,29} (~23 μm). On the other hand, *in situ* synthesised TiC_x particles have a good interface bonding between particles and the matrix.

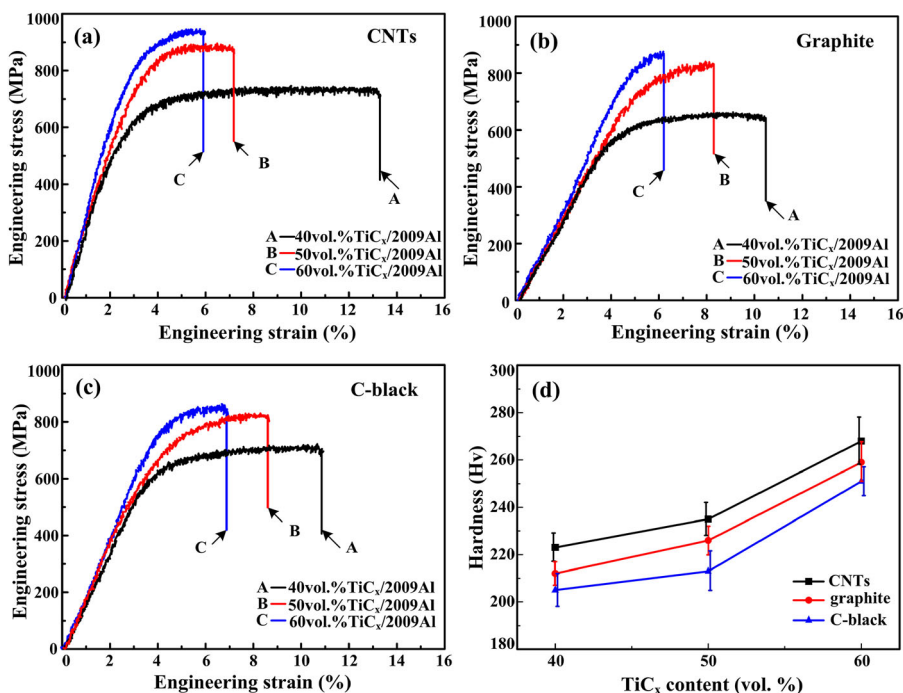


3 SEM images of the samples of 40, 50 and 60 vol.-%TiC_x/2009Al composites fabricated by using a–c CNTs, d–f graphite and g–i C-black as carbon source

In situ synthesised finer TiC_x particles with spherical shape and good particles-matrix interface can dramatically reduce stress concentration and crack propagation. Hence, the composites are effectively strengthened.

The typical microscopic fracture morphologies of 40–60 vol.-% TiC_x/2009Al composites fabricated by using CNTs are shown in Fig. 5a–c. It can be seen that the fracture surfaces of 40 and 50 vol.-% TiC_x/Al composites

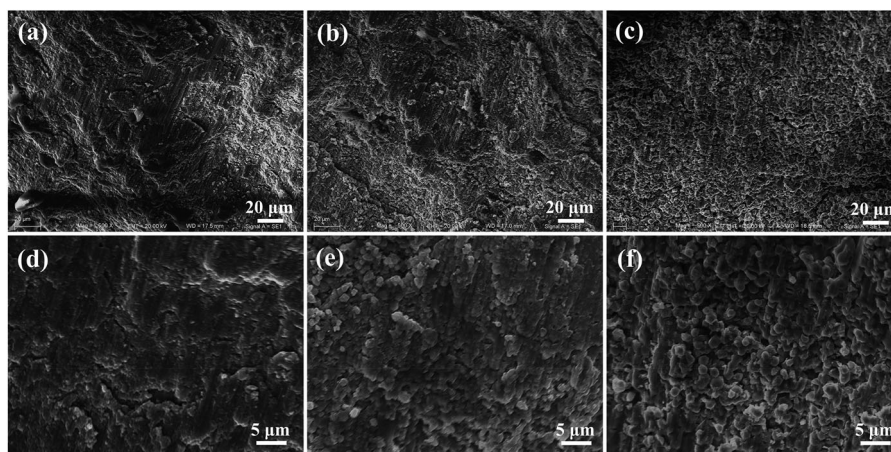
shows some dimples, while that of 60 vol.-% TiC_x/Al composite is relatively flat. The higher hardness of finer-sized particle can accumulate slip bands to improve the plasticity.³⁰ Further study of the compression fracture surfaces of the corresponding composites with high-magnified SEM images is showed in Fig. 5d–f, which suggests that the debonding between the synthesised TiC_x particles and aluminium matrix is the main fracture mode in the



4 Compression engineering stress–strain curves of 40, 50 and 60 vol.-%TiC_x/2009Al composites fabricated by using a CNTs, b graphite and c C-black as carbon source, d micro-hardness of corresponding composites

Table 1 The compression test data of 40–60 vol.-%TiC_x/2009Al composites

C source	40 vol.-%TiC _x /2009Al			50 vol.-%TiC _x /2009Al			60 vol.-%TiC _x /2009Al		
	$\sigma_{0.2}$ /MPa	σ_{UCS} /MPa	ϵ /%	$\sigma_{0.2}$ /MPa	σ_{UCS} /MPa	ϵ /%	$\sigma_{0.2}$ /MPa	σ_{UCS} /MPa	ϵ /%
CNTs	514 ⁺⁹ ₋₈	733 ⁺⁷ ₋₅	10.4 ^{+1.4} _{-0.5}	701 ⁺⁵ ₋₅	907 ⁺⁴ ₋₆	4.1 ^{+1.8} _{-0.5}	722 ⁺⁷ ₋₆	946 ⁺⁹ ₋₅	3.2 ^{+0.8} _{-0.2}
Graphite	483 ⁺⁷ ₋₃	644 ⁺⁵ ₋₉	6.6 ^{+0.6} _{-0.7}	608 ⁺⁶ ₋₇	812 ⁺⁷ ₋₂	3.4 ^{+1.0} _{-0.4}	656 ⁺⁵ ₋₄	849 ⁺⁶ ₋₅	1.9 ^{+0.3} _{-0.9}
C-black	491 ⁺⁵ ₋₂	715 ⁺⁴ ₋₃	7.0 ^{+0.9} _{-0.3}	637 ⁺⁸ ₋₇	818 ⁺⁵ ₋₆	4.6 ^{+0.9} _{-0.7}	664 ⁺⁸ ₋₅	834 ⁺⁷ ₋₂	2.7 ^{+0.5} _{-0.8}

**5** a–c SEM images of fracture surfaces of 40, 50 and 60 vol.-% TiC_x/2009Al composites fabricated by using CNTs as carbon source, d–f high-magnified SEM images of the corresponding composite

high-volume-fraction TiC_x/2009Al composites. When the TiC_x contents are 40 and 50 vol.-%, the aluminium in composites is abundant and can bond with the TiC_x particles tightly, as shown in Fig. 5d and e. With increasing TiC_x content, as shown in Fig. 5f, the aluminium reduces and is too little to bond with the TiC_x particles sufficiently. Thus the strength of the composites is mainly determined by TiC_x content and bonding strength between the particles and aluminium matrix. In addition, the reducing of aluminium content in the composites increases the brittleness of the composites, thus leading to the decrease in ϵ_f of the composites with increasing TiC_x particles content.

Conclusion

By using CNTs, graphite and C-black as carbon sources, 40–60 vol.-% TiC_x/2009Al composites were successfully fabricated by the combination of combustion synthesis and vacuum hot press.

- (i) When CNTs and C-black were used, the synthesised TiC_x with particles sizes of 0.08–1 and 0.9–5 μm, respectively, was spherical or nearly spherical in shape. While graphite was used, the synthesised TiC_x with particles sizes of 0.2–2 μm was octahedral or spherical in shape.
- (ii) All of the $\sigma_{0.2}$, σ_{UCS} and hardness of TiC_x/2009Al composites increased with increasing TiC_x content, while the ϵ decreased. Among them, the 60 vol.-% TiC_x/2009Al composites fabricated by using CNTs as carbon source had the highest σ_{UCS} and hardness (~946 MPa, 260 ± 10 Hv), which were 11.4% and 3.4%, 13.4% and 7.5%

higher than those of composites fabricated by using graphite and C-black as carbon sources.

- (iii) Finer-sized TiC_x particles with spherical shape could dramatically reduce stress concentration and crack propagation, and increase bonding strength between the particles and aluminium matrix, leading to the strength increase of the composites.

Acknowledgements

This work is supported by the National Natural Science Foundation of China (NNSFC, No. 51571101), National Basic Research Program of China (973 Program, No. 2012CB619600), the Project supported by the 'twelfth five-year plan' Science & Technology Research Foundation of Education Bureau of Jilin Province, China (Grant No. 2015-479), National Natural Science Foundation of China (No. 51601066 and 51501176), Project (No. 2016174) supported by Graduate Innovation Fund of Jilin University and the Project 985-High Properties Materials of Jilin University.

ORCID

Q.-L. Zhao  <http://orcid.org/0000-0002-7124-4032>

References

1. F. Akhtar, S. J. Askari, K. A. Shah, X. L. Du and S. J. Guo: 'Microstructure, mechanical properties, electrical conductivity and wear behavior of high volume TiC reinforced Cu-matrix composites', *Mater. Charact.*, **2009**, *60*, (4), 327–336.

2. B. G. Kim, S. L. Dong and S. D. Park: 'Effects of thermal processing on thermal expansion coefficient of a 50 vol. % SiCp/Al Composite', *Mater. Chem. Phys.*, **2001**, **72**, (1), 42–47.
3. I. H. Song, D. K. Kim and Y. D. Hahn: 'The effect of a dilution agent on the dipping exothermic reaction process for fabricating a high-volume TiC-reinforced aluminum composite', *Scripta Mater.*, **2003**, **48**, (4), 413–418.
4. Q.-Q. Xuan, S.-L. Shu, F. Qiu, S.-B. Jin and Q.-C. Jiang: 'Different strain-rate dependent compressive properties and work-hardening capacities of 50vol% TiC_x/Al and TiB₂/Al composites', *Mater. Sci. Eng. A.*, **2012**, **538**, 335–339.
5. A. B. Pandey, R. S. Mishra and Y. R. Mahajan: 'Effect of isothermal heat treatment on the creep behaviour of an Al-TiC_p composite', *Mater. Sci. Eng. A.*, **1996**, **206**, (2), 270–278.
6. Ö. N. Doğan, J. A. Hawk, J. H. Tylczak, R. D. Wilson and R. D. Govier: 'Wear of titanium carbide reinforced metal matrix composites', *Wear*, **1999**, **225–229**, 758–769.
7. E. Candan, H. Ahlatci and H. Çimenoglu: 'Abrasive wear behaviour of Al-SiC composites produced by pressure infiltration technique', *Wear*, **2001**, **247**, (2), 133–138.
8. H. Ahlatci, E. Candan and H. Çimenoglu: 'Abrasive wear behavior and mechanical properties of Al-Si/SiC composites', *Wear*, **2004**, **257**, (5), 625–632.
9. L.-J. Zhang, Q.-Q. Xuan, J.-G. Wang, F. Qiu and Q.-C. Jiang: 'Effects of TiB₂ content and alloy elements (Mg, Mo, V) on the compression properties of high-volume-fraction TiB₂/Al composites', *Mater. Sci. Eng. A.*, **2014**, **607**, 28–32.
10. F. Qiu, Y. Y. Gao, J. Y. Liu, S. L. Shu, Q. Zou, T. Z. Zhang and Q. C. Jiang: 'Effect of C/Ti ratio on the compressive properties and wear properties of the 50 vol.% submicronized TiC_x/2014Al composites fabricated by combustion synthesis and hot press consolidation', *Powder Metall.*, **2016**, **59**, (4), 256–261.
11. B. H. Li, Y. Liu, J. Li, H. Cao and L. He: 'Fabrication of *in situ* TiB₂-TiC reinforced steel matrix composites by spark plasma sintering', *Powder Metall.*, **2011**, **54**, (3), 222–224.
12. A. Kumar, M. M. Mahapatra and P. K. Jha: 'Effect of machining parameters on cutting force and surface roughness of *in situ* Al-4.5% Cu/TiC metal matrix composites', *Measurement*, **2014**, **48**, 325–332.
13. D. Strzeczewski, Z. Wokulski and P. Tkacz: 'Growth and TEM and HREM characterization of TiC crystals grown from high-temperature solutions', *Cryst. Res. Technol.*, **2003**, **38**, (3–5), 283–287.
14. M. Kouzeli, L. Weber, C. San Marchi and A. Mortensen: 'Influence of damage on the tensile behaviour of pure aluminium reinforced with ≥40 vol. pct alumina articles', *Acta Mater.*, **2001**, **49**, (18), 3699–3709.
15. V. A. Romanova, R. R. Balokhonov and S. Schmauder: 'The influence of the reinforcing particle shape and interface strength on the fracture behavior of a metal matrix composite', *Acta Mater.*, **2009**, **57**, (1), 97–107.
16. S. C. Tjong and Z. Y. Ma: 'Microstructural and mechanical characteristics of *in situ* metal matrix composites', *Mater. Sci. Eng. R.*, **2000**, **29**, (3), 49–113.
17. S. B. Jin, P. Shen, D. S. Zhou and Q. C. Jiang: 'Self-propagating high-temperature synthesis of Nano-TiC_x particles with different shapes by using carbon nano-tube as C source', *Nanoscale Res. Lett.*, **2011**, **6**, (1), 1–7.
18. M. S. Song, M. X. Zhang, S. G. Zhang, B. Huang and J. G. Li: 'In situ fabrication of TiC particulates locally reinforced aluminum matrix composites by self-propagating reaction during casting', *Mater. Sci. Eng. A.*, **2008**, **473**, (1), 166–171.
19. Y. Choi and S.-W. Rhee: 'Effect of carbon sources on the combustion synthesis of TiC', *J. Mater. Sci.*, **1995**, **30**, (18), 4637–4644.
20. P. Yu, L. C. Zhang, W. Y. Zhang, J. Das, K. B. Kim, J. Eckert: 'Interfacial reaction during the fabrication of Ni₆₀Nb₄₀ metallic glass particles-reinforced Al based MMCs', *Mater. Sci. Eng. A.*, **2007**, **444**, (1), 206–213.
21. M. S. Song, B. Huang, M. X. Zhang and J. G. Li: 'Study of formation behavior of TiC ceramic obtained by self-propagating high-temperature synthesis from Al-Ti-C elemental powders', *Int. J. Refract. Met. Hard Mater.*, **2009**, **27**, (3), 584–589.
22. W.-C. Lee and S.-L. Chung: 'Ignition phenomena and reaction mechanisms of the self-propagating high-temperature synthesis reaction in the Ti+C system', *J. Mater. Sci.*, **1995**, **30**, (6), 1487–1494.
23. E.-L. Zhang, S.-Y. Zeng, Q.-C. Li, B. Yang and M.-Z. Ma: 'A study on the kinetic process of reaction synthesis of TiC: part I. experimental research and theoretical model', *Metall. Mater. Trans. A.*, **1999**, **30**, (4), 1147–1151.
24. S.-B. Jin, P. Shen, B.-L. Zou and Q.-C. Jiang: 'Morphology evolution of TiC_x grains during SHS in an Al-Ti-C System', *Cryst. Growth Des.*, **2009**, **9**, (2), 646–649.
25. M. S. Song, B. Huang, Y. Q. Huo, S. G. Zhang, M. X. Zhang, Q. D. Hu and J. G. Li: 'Growth of TiC octahedron obtained by self-propagating reaction', *J. Cryst. Growth*, **2009**, **311**, (2), 378–382.
26. J.-C. Charlier: 'Defects in carbon nanotubes', *Acc. Chem. Res.*, **2002**, **35**, (12), 1063–1069.
27. S. Ehtemam-Haghighi, Y. Liu, G. Cao, L. C. Zhang: 'Phase transition, microstructural evolution and mechanical properties of Ti-Nb-Fe alloys induced by Fe addition', *Mater. Des.*, **2016**, **97**, 279–286.
28. Z. H. Tan, B. J. Pang, D. T. Qin, J. Y. Shi and B. Z. Gai: 'The compressive properties of 2024Al matrix composites reinforced with high content SiC particles at various strain rates', *Mater. Sci. Eng. A.*, **2008**, **489**, (1), 302–309.
29. H. Ahlatci, E. Candan and H. Çimenoglu: 'Mechanical properties of Al-60 Pct SiC_p composites alloyed with Mg', *Metall. Mater. Trans. A.*, **2004**, **35**, (7), 2127–2141.
30. L. C. Zhang, J. Das, H. B. Lu, C. Duhamel, M. Calin, J. Eckert: 'High strength Ti-Fe-Sn ultrafine composites with large plasticity', *Scripta Mater.*, **2007**, **57**, (2), 101–104.